Received: 19 March 2024 | Accepted: 16 October 2024 | Published online: 12 November 2024

DOI: 10.1002/jeq2.20652

Journal of Environmental Quality

TECHNICAL REPORT

Emerging Contaminants

Effect of gypsum on transport of IMX-104 constituents in overland flow under simulated rainfall

Viktor Polyakov[1] | Samuel Beal[2] | Stephen Mercer Meding[3] | Katerina Dontsova[3,4]

[1]USDA-ARS, Southwest Watershed Research Center, Tucson, Arizona, USA

[2]U.S. Army Engineer Research and Development Center, CRREL, Hanover, New Hampshire, USA

[3]Biosphere 2, University of Arizona, Oracle, Arizona, USA

[4]Department of Environmental Science, University of Arizona, Tucson, Arizona, USA

Correspondence
Viktor Polyakov, USDA-ARS, Southwest Watershed Research Center, 2000 E Allen Rd., Tucson, AZ 85718, USA.
Email: viktor.polyakov@usda.gov

Assigned to Associate Editor William Strosnider.

Funding information
Strategic Environmental Research and Development Program, Grant/Award Number: ER19-1074

Abstract

Residue of energetic formulations, which is deposited on military training grounds following incomplete detonation, poses biotic hazards. This residue can be transported off-site, adsorb to soil clays and organic matter, transform or degrade, or taken up by plants and animals. Its harmful effects can be mitigated by localizing the energetics at the site of initial deposition using soil amendments and allowing them to bio- and photodegrade in situ. Small plots with coarse loamy soil were used to study the effect of gypsum ($CaSO_4{\cdot}2H_2O$) on transport and redistribution under simulated rainfall of various sizes of insensitive munition explosive (IMX)-104 particles, which consist of 3-nitro-1,2,4-triazol-5-one (NTO), 2,4-dinitroanisole (DNAN), hexahydro-1,3,5-trinitro-1,3,5-triazine (RDX), and octahydro-1,3,5,7-tertranitro-1,3,5,7-tetrazocine (HMX). The addition of gypsum more than doubled infiltration and decreased sediment loss by 16% compared to the control. The post-rainfall mass balance of IMX-104 in the order from greater to smaller pools was as follows: (1) soil surface retention, (2) off-site loss to overland flow, and (3) sub-surface infiltration. Overall, the application of gypsum significantly decreased concentration and the total mass loss of dissolved DNAN, RDX, and HMX in surface runoff. In addition, gypsum significantly decreased (for NTO, DNAN, and HMX) or delayed (for NTO, DNAN, RDX, and HMX) the peak discharge of <2 mm particulate energetics. The infiltration of NTO in the gypsum treatment was fivefold greater than in the control. Moreover, DNAN and RDX were also present in infiltration, while in the gypsum-free control none were found. Gypsum shifted the total mass balance of energetics toward subsurface flow. This study indicates that gypsum may decrease off-site transport of energetic constituents in the soils that are subject to surface sealing.

Abbreviations: DNAN, 2,4-dinitroanisole; HMX, octahydro-1,3,5,7- tertranitro-1,3,5,7-tetrazocine; HPLC, high precision liquid chromatography; IMX, insensitive munition explosive; NTO, 3-nitro-1,2,4-triazol-5-one; RDX, hexahydro-1,3,5-trinitro-1,3,5-triazine; RO, reverse osmosis; WGRS, Walnut Gulch Rainfall Simulator; XS, extra small.

Plain Language Summary

This study investigates gypsum soil amendment as a method to diminish off-site contamination by munition energetics. These energetics, originating from residues of low-order detonations on military training grounds, are hazardous for the environment. This research examined mitigating effects of gypsum on rainfall-driven transport of IMX-104 components (NTO, DNAN, RDX, and HMX) including in runoff, infiltration, and sediment. The results have implications for risk assessment and land management.

1 | INTRODUCTION

Military grounds used for training activities experience a wide range of environmental stresses, including contamination by energetic formulations contained in munitions. Among these is insensitive munition explosive (IMX)-104, composed of 2,4-dinitroanisole (DNAN), 3-nitro-1,2,4-triazol-5-one (NTO), hexahydro-1,3,5-trinitro-1,3,5-triazine (RDX), and HMX (octahydro-1,3,5,7- tertranitro-1,3,5,7-tetrazocine) (Singh et al., 2010). When munitions malfunction and fail to fully detonate, IMX-104 residue is scattered and deposited on the soil surface (Bigl et al., 2021; Walsh et al., 2014).

This residue poses environmental risk due to low to moderate toxicity of its constituents, particularly DNAN and RDX, for aquatic species and mammals (Gust et al., 2018; Lent, 2019; Lotufo et al., 2018). The effects include but are not limited to tissue damage, impaired metabolism, and inflammatory processes. After the deposition, energetic compounds can follow different transport pathways and experience transformation under environmental impacts or artificial treatments (Brooks et al., 2003). The particles can further mechanically breakup, dissolve (Fuller et al., 2012; Taylor et al., 2015), components can reversibly adsorb to soil clays and organic matter (Arthur et al., 2017; Dontsova et al., 2009; Hawari et al., 2015), bio- and photodegrade (Dontsova et al., 2020, 2023; Qin et al., 2021), or be taken up by plants (Price et al., 2011).

Table 1 shows the structures and relevant properties of the studied compounds. DNAN is a nitroaromatic compound, while RDX and HMX are nitramines. DNAN, RDX, and HMX are polar but non-ionic, while NTO is anionic at environmental pH range with pKa of 3.76 (Nandi et al., 2013). NTO has the highest water solubility and low adsorption potential in soils, while DNAN, RDX, and HMX (in decreasing order) have lower solubilities and higher affinity for soils.

Rainfall stands out as one of the key drivers of energetics mobilization and redistribution on the landscape. Taylor et al. (2009) studied simulated rainfall-driven dissolution of energetics as a function of particle size, particle composition, and rainfall rate. They described dissolution interaction and controls between components with different solubility (RDX, TNT, HMX, and others). Raindrops can break up coarser energetic particles, facilitating their mechanical transport and dissolution (Fuller et al., 2015). Price et al. (2011) studying the effect of vegetation on transport of energetics under rainfall described how soil chemical and physical properties, plant uptake, and seasonal variations control movement of RDX, HMX, and TNT in surface runoff. Polyakov et al. (2023) and Karls et al. (2023) studied transport of IMX-104 on plots under simulated rainfall and in eroding rills. The authors provided complete mass balance of energetics and identified their major transport pathways: loss to runoff in dissolved and particulate form, infiltration, and retention in situ. They described relationships between the loss of energetics and their particle size, and the rates of runoff, rainfall, and erosion. Particularly, Polyakov et al. (2023) demonstrated that runoff and sediment yield positively correlated with loss of IMX-104 constituents in overland flow.

Several methods have been used to decrease soil erosion and sediment movement subject to rainfall. Among them are soil amendments, particularly gypsum ($CaSO_4 \cdot 2H_2O$), which is a well-established practice in agriculture (Norton & Dontsova, 1998; Shainberg et al., 1989; Zoca & Penn, 2017). Gypsum has relatively high solubility (0.0153 mol L^{-1}) (Charola et al., 2007) and dissolves in soil increasing ionic strength of the pore water and supplying exchangeable Ca to clay exchange complex (Dontsova & Norton, 2002; Favaretto et al., 2006) thus reducing soil dispersion. This in turn increases infiltration (Miller, 1987), lessens surface sealing and crusting, and decreases soil loss (Peterson et al., 2002; Truman et al., 2010; Wallace et al., 2001). Application of gypsum has been shown to abate transport of phosphorus (Torbert & Watts, 2014; Zhu & Alva, 1994), nitrogen (Favaretto et al., 2006), and other nutrients (Kumar & Saha, 2011). At the same time, solution of gypsum in equilibrium with pure water has circumneutral pH (6.7) and is not likely to have a direct effect on other chemical properties of the soil or on studied compounds.

Therefore, this study examined an approach to decrease transport in overland flow that would allow mitigating negative off-site effects of energetic formulations by containing them in the place of initial deposition and allowing them to bio- and photodegrade in situ. The specific goals of this research were to: (a) evaluate the effectiveness of a common soil amendment (gypsum) in reducing the loss of IMX-104 from the soil surface and (b) quantify the effect of gypsum on redistribution of IMX-104 components among different transport pathways.

Core Ideas

- The study quantifies the effect of surface applied gypsum on transport of insensitive munition explosive (IMX)-104 under artificial rainfall.
- The mobility of IMX-104 energetics components is controlled by their solubility and particle size.
- Application of gypsum decreased concentration and the total mass of dissolved energetics in the surface runoff.
- Gypsum facilitated redistribution of mobilized energetics into the subsurface flow.

2 | METHODS

2.1 | Instrumentation and materials

The materials and procedure in this experiment were similar to that described in Polyakov et al. (2023). The soil was collected on the grounds of the Arizona National Guard Florence Military Reservation from 0.15 top layer. The soil is classified as Laveen loam, coarse-loamy, mixed, superactive, hyperthermic Typic Haplocalcids and contains 29% clay, 14.2% silt, and 56.8% sand. Its organic carbon content was 0.3%, cation exchange capacity (CEC) 13.7 $cmol_c\ kg^{-1}$, specific surface area 33.0 $m^2\ g^{-1}$, electrical conductivity (EC) of 1:1 suspension was 252 $\mu S\ cm^{-1}$, and pH 8.3. Prior to the experiment, the soil was air dried and sieved to 5 mm.

The energetic formulation used in the experiment, IMX-104, is a melt cast mixture of NTO, RDX, and HMX in DNAN (Table 1). Samples of IMX-104 particles were collected at the site of low-order detonation tests on frozen surfaces at Joint Base Elmendorf-Richardson and at Donnelly Training Area in Alaska as a part of the Environmental Security Technology Certification Program project ER18-5105. The methodology adapted from Walsh et al. (2017) was as follows: mortar rounds containing IMX-104 were initiated using a reduced mass fuze booster (composition C-4) over a cleared ice surface, and distributed particles were collected from the ice surface at distances between 0 and 20 m around the detonation center. After freeze drying, samples were initially dry sieved to 2 mm, and then the larger fraction refined through sieving at 9.51, 4.75, and 2.83 mm. The energetic purity of the study materials was ensured visually for the >2 mm size fractions and by high-performance liquid chromatography (HPLC) for the <2 mm size fraction (96.6% for the study sample; Beal and Bigl (2022). These four energetic particle fractions (9.51–4.75 or large [L], 4.75–2.83 or medium [M], 2.83–2 mm or small [S], and <2 mm, or extra small [XS]) were used in this rainfall simulation study. Gypsum powder ($CaSO_4{\cdot}2H_2O$) with ≥98% purity (Thermo Scientific Chemicals, catalog # 315255000) was used as a soil amendment treatment.

The experimental plots consisted of four stainless steel boxes (0.45 m long, 0.32 m wide, and 0.20 m deep) equipped with a spillway, drainage holes, and 0.2-m tall splash screens along the perimeter (Bradford et al., 1987). The boxes were mounted on stands that allowed slope adjustment. The water table in the boxes was controlled via height-adjustable communicating vessel connected to drainage openings (Figure 1). The artificial rainfall was generated using a Walnut Gulch Rainfall Simulator (WGRS) (Paige et al., 2004). This simulator is equipped with variable-speed oscillating spray nozzles, which allow uniform rainfall coverage over 12 m^2 area. The WGRS can deliver precipitation rates from 12 to 180 mm h^{-1} with 204 kJ $ha^{-1}\ mm^{-1}$ kinetic energy and from 0.29 to 7.2 mm drop size. This closely mimics the characteristics of natural rainfall, making the WGRS well suited for a wide variety of water erosion and transport experiments (Polyakov et al., 2018; Zhang et al., 1998a).

2.2 | Experimental procedure

Prior to the experiment the WGRS was calibrated using a set of rain gauges arranged in a grid pattern. This insured that each plot received the same amount of rainfall. The amount of rain falling on the spillway was measured, accounted for as dilution, and excluded from further calculations. Four plots were used simultaneously during a single simulation.

The boxes were filled with layers of gravel (13 cm), sand (3 cm), and soil (4 cm) each separated by nylon mesh. The sand was Ottawa F-75 whole grain silica with >99% purity (U.S. Silica Company). To ensure uniform density and replicability, all materials were added in small increments and compacted in between. The weight of soil in the box was recorded. Approximately 1 h before the rainfall, the soil was saturated with reverse osmosis (RO)-treated water through the drainage tubes from below, then the plots were tilted to 5% slope with water table set 5 cm below the surface at the center

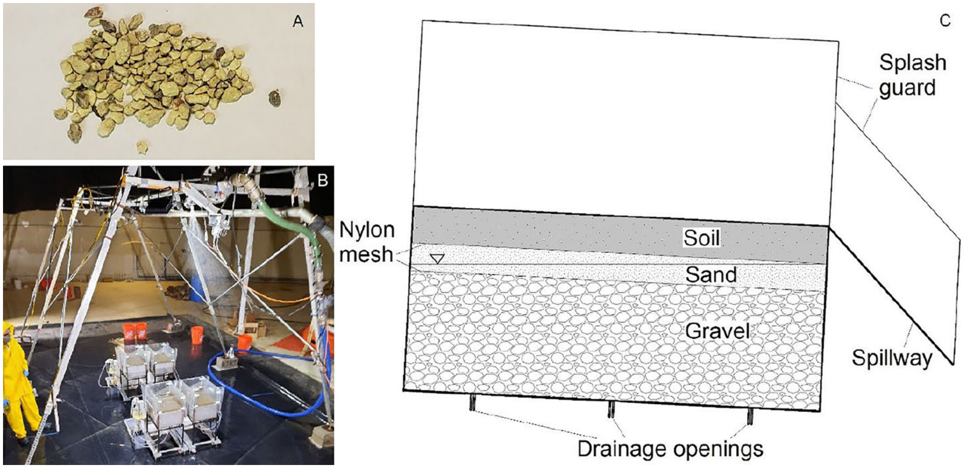

FIGURE 1 Insensitive munition explosive (IMX)-104 material in 2.83–4.75 mm size (A), rainfall simulation setup (B), and cross section of the experimental plot (C).

of the plot. Four rain gauges were attached on the outside of each plot as a check.

All the treatments (control and gypsum) received 1.00 g of IMX-104 from one of the four size fractions. It was evenly spread across the soil surface. The size fraction allocation to each plot was assigned randomly. The gypsum treatment consisted of surface application of 72 g of $CaSO_4{\cdot}2H_2O$ per plot, an equivalent of field application of 5 Mg ha^{-1} (Lee et al., 2010; Miller, 1987). Both IMX-104 and gypsum were applied immediately before the rainfall. Each treatment was replicated three times resulting in 24 simulation plots in total.

Rainfall was applied for 60 min at 52 mm h^{-1} intensity using RO water. The entire runoff from the plots was collected into 1-L glass jars replaced every 5 min (12 samples per plot). Infiltration samples were collected as overflow from the vessels controlling the water table. Infiltration samples were obtained synchronously with the runoff, weighed individually, and combined into a composite sample (one per plot) for further analysis.

After the simulation, the soil remaining in the boxes was collected in three discrete layers: 0–1 cm, 1–2 cm, and 2–4 cm. Soil splash from spillway and screens was collected and added to the 0- to 1-cm layer sample. After that, the boxes were drained overnight and the drainage collected. The sand from the bottom of the box was discarded, and gravel and mesh were washed and reused in the next simulation.

2.3 | Laboratory procedures and data analysis

Runoff samples were weighed and a 30 mL subsample was centrifuged in 30-mL Kimble clear borosilicate glass vials (Vineland, New Jersey) at 3400 g (4500 rpm) for 20 min. Then 2 mL of the supernatant was filtered through 0.45 µm polyvinyl difluoride syringe filter and analyzed using HPLC to determine concentrations of energetics. The rest of supernatant from the Kimble vials was discarded and the sediment pellet retained. Next day, after settling overnight, the remaining supernatant from 1-L jars was transferred into 750-mL Teflon bottles and centrifuged at the same settings, while bulk of sediment that settled in 1-L jars was combined with sediment from the previous day in the same 30-mL vials. The pellet from Teflon bottle was also transferred to the same 30-mL vials. Then the vials were centrifuged again in order to separate and discard any remaining rainwater supernatant.

The sediment samples were extracted in a two-step method by Crouch et al. (2020). First, methanol was added to the sediment at 5:1 weight ratio, equilibrated on a shaker for 24 h, and centrifuged as described previously. Then the supernatant was subsampled (2 mL) and its excess decanted. After that methanol:water mixture (1:1 by volume) was added to the remaining sediments and equilibration, centrifugation, and subsampling (2 mL) repeated. The extracts were analyzed by HPLC. The sediment in the vials was then dried at 110˚C and weighed to determine sediment yield from the plots.

The top (0–1 cm) soil layer from the plots potentially contained IMX-104 particles. In order to homogenize it, the soil was air dried and milled following Environmental Protection Agency method 8330B (USEPA, 2006). The two lower layers (1–2 cm and 2–4 cm) were thoroughly mixed without grinding, assuming they could only contain dissolved energetic components. The three layers were subsampled in triplicate (5 g each) and then extracted and analyzed same as the sediment.

The extracts and runoff were analyzed using Dionex Ultimate 3000 HPLC by Thermo Fisher Scientific Inc. NTO concentration was measured with Hypercarb column, 75:25 acetonitrile:water mobile phase with 0.1% trifluoroacetic acid (TFA) at 1 mL min^{-1} isocratic for 3 min at 32˚C, and detected

TABLE 1 Chemical characteristics of insensitive munition explosive (IMX)-104 constituents. The values are molecular weight (MW), solubility at 25˚C, octanol-water partitioning coefficient (log K_{ow}), soil organic carbon-water partitioning coefficient (log K_{OC}), and measured or estimated adsorption coefficient (K_d) for Florence soil used in this study.

Compound	Formula	Structure	MW	Solubility	Log K_{ow}	Log K_{oc}	K_d (L kg^{-1})
NTO 3-nitro-1,2,4-triazol-5-one	$C_2H_2N_4O_3$	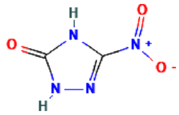	130.01	16,642[a]	0.37–1.03[b]	0.6–1.79[a]	0.06[a]
DNAN 2,4-dinitroanisole	$C_7H_6N_2O_5$	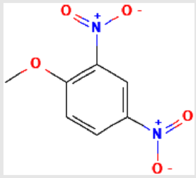	198.03	276.2[c]	1.61[b]	1.93–2.63[d], 3.11[c]	1.90[d]
RDX hexahydro-1,3,5-trinitro-1,3,5-triazine	$C_3H_6N_6O_6$	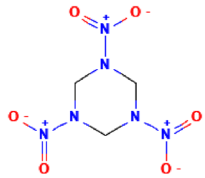	222.03	56.35[e]	0.81–0.87[f]	0.88–2.4[g]	0.82[h]
HMX octahydro-1,3,5,7-tertranitro-1,3,5,7-tetrazocine	$C_4H_8N_8O_8$	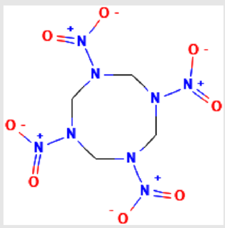	296.05	4.46[e], 5[i]	0.06[j], 0.19[k], 0.26	2.8[g], 0.54[i]	1.03[g]

[a]Mark et al. (2016)
[b]Sokkalingam et al. (2008)
[c]Boddu et al. (2008)
[d]Arthur et al. (2017)
[e]Monteil-Rivera et al. (2004)
[f]Yoon et al. (2005)
[g]Brannon and Pennington (2002)
[h]Tucker et al. (2002)
[i]ATSDR (1997)
[j]ATSDR (2012)
[k]Yoon et al. (2002)

at 2.5 min and 315 nm (Le Campion et al., 1999). DNAN and its transformation products, as well as RDX, and HMX were measured with Acclaim reverse phase C18 column, 5 µm particle size, 43:57 methanol:water mobile phase with 1 mL min^{-1} flow rate for 30 min. DNAN was detected at 21 min and 300 nm, RDX at 8 min and 254 nm, and HMX at 5 min and 254 nm. All samples were refrigerated before HPLC analysis.

The experiment utilized a randomized complete block design. Analysis of variance and *t*-test (where appropriate) were used to compare runoff, soil erosion, and loss of energetic compounds across treatments and energetic particle sizes. Data processing and statistical analyses were performed using MS Excel and SAS statistical software (SAS Institute). Statistical significance is reported at $p = 0.05$.

3 | RESULTS AND DISCUSSION

3.1 | Runoff, infiltration, and sediment yield

During the course of the simulations only sheet flow was observed on the soil surface and no rill development or scour occurred. The infiltration and runoff were nearly steady throughout the duration of the rain, except for the first 10 min, during which the surface was being saturated and ponding was developing (Figure 2). The total infiltration in the gypsum treatment (4.3 mm) was 55% greater than in control (2.8 mm) and the difference was statistically significant. A small 4.5% increase in runoff was also observed in the gypsum treatment (55.1 mm) compared to the control (52.8 mm). However, this

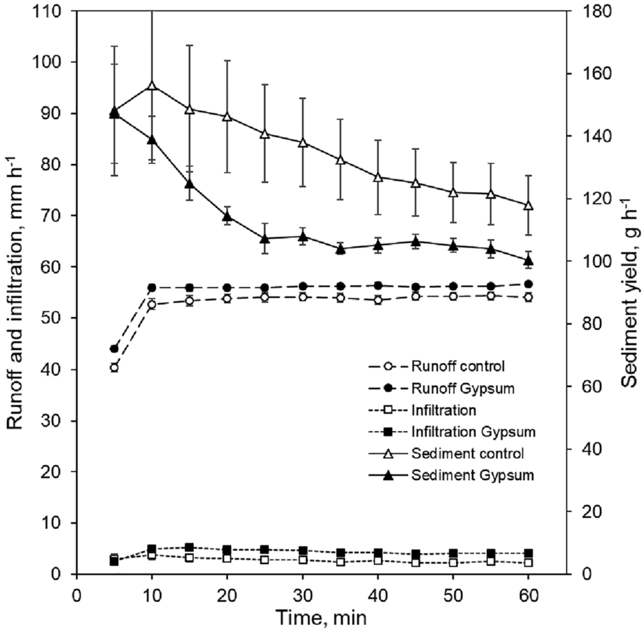

FIGURE 2 Runoff, infiltration, and soil loss from the plots with gypsum treatment and control (standard error bars, $n = 12$).

difference was attributed to the variability of rainfall input, which lies within the range of simulator precision (Paige et al., 2004), and is unlikely to appreciably affect infiltration rate or flow transport capacity.

The soil loss varied greatly through the duration of rainfall. On control plots it peaked at 156 g h^{-1} 10 min after start of experiment and then declined steadily to 118 g h^{-1}. This was likely due to progressive loss of fine and loose particles and continuous soil compaction by raindrops. This trend is consistent with sediment dynamics observed on larger field plots and slopes, particularly those with poorly aggregated soil (Li et al., 2020; Parsons et al., 1991). In the gypsum treatment the initial soil loss rate was similar to control (147 g h^{-1}). However, it quickly declined and after 25 min of simulation approached approximately steady rate of 100–107 g h^{-1}, a 32% decrease. For comparison, on the control the steady rate was 117–121 g h^{-1}, a decrease of 20%. The average total sediment yield from control plots was 135.3 versus 113.8 g from the gypsum treatment (an equivalent of 9.4 and 7.9 t ha^{-1}, respectively). Although this was a 16% decline for the treated plots, the difference was not statistically significant.

Our observations were consistent with a similar plot study (Favaretto et al., 2006) where gypsum amendment increased infiltration by 145%–157%, while the decrease of sediment yield was moderate and not statistically significant (21%–34%), particularly at high 60 mm h^{-1} rainfall rates. Raindrop detachment and sheet flow are the key drivers for inter-rill sediment delivery (Abrahams & Parsons, 1994; Bradford et al., 1987; Zhang et al., 1998b). By inhibiting soil dispersion gypsum acts to redistribute water toward infiltration thus hindering overland sediment transport (Shainberg et al., 1989). In our experiment the relative weight of infiltration (<7%) in the water balance was too small to significantly affect overland flow, although the initial drop in sediment yield in the gypsum treatment was well pronounced (Figure 2).

3.2 | Effect of gypsum on surface transport dynamics of NTO, DNAN, and RDX

The concentrations of all energetics dissolved in runoff during the simulation event showed a declining temporal trend on both treatments (Figure 3). The concentrations for all compounds and particle fractions peaked at 5–10 min of rainfall and later approached steady-state values.

The greatest initial concentrations were observed on plots with XS particles. Namely, in the control treatment, NTO, DNAN, and RDX concentrations were 335, 26, and 5 mg L^{-1}, respectively, which reflects the individual solubility of the compounds (Table 1). These values were fivefold to 20-fold greater than those from plots with S, M, and L particles. Runoff from XS particles have also shown a more rapid concentration decline over time than from other fractions. This pattern was attributed to two processes occurring simultaneously. First, the dissolution rate of smaller IMX-104 particles is greater because it is directly proportional to the surface area (Dontsova et al., 2023). Second, finer particles are more readily transported off site, and thus cease being an in situ source of solute. On the other hand, larger particles, while dissolving slower, are less mobile and can release energetics into the flow over a longer period.

The dissolved transport dynamic was similar for both treatments (Figure 3). However, runoff from the gypsum treatment with XS particles had significantly lower initial concentrations for all energetics compounds (NTO, DNAN, RDX, and HMX) compared to the control (Figure 3). While presence of inorganic salts in solution can inhibit dissolution of organic compounds in water, "salting-out effect" (Schwarzenbach et al., 2003) when present at solubility limit, gypsum would not be expected to decrease solubility of studied organics by more than 1% (Boddu et al., 2008). Although the concentration of energetics in bulk samples were below their solubility limits (Table 1), it is likely that local concentrations in runoff in the vicinity of source particles were higher. However, the decrease in solution transport in the gypsum treatment is most likely related to the decrease in movement of XS particles with erosion. As a result, in the gypsum treatment, particularly on XS plots, it took longer for concentrations to reach a steady state (Figure 3). For example, on the control treatment NTO concentration (XS) was below detection limit by 45 min, while in gypsum it was statistically above detection limit during the entire event.

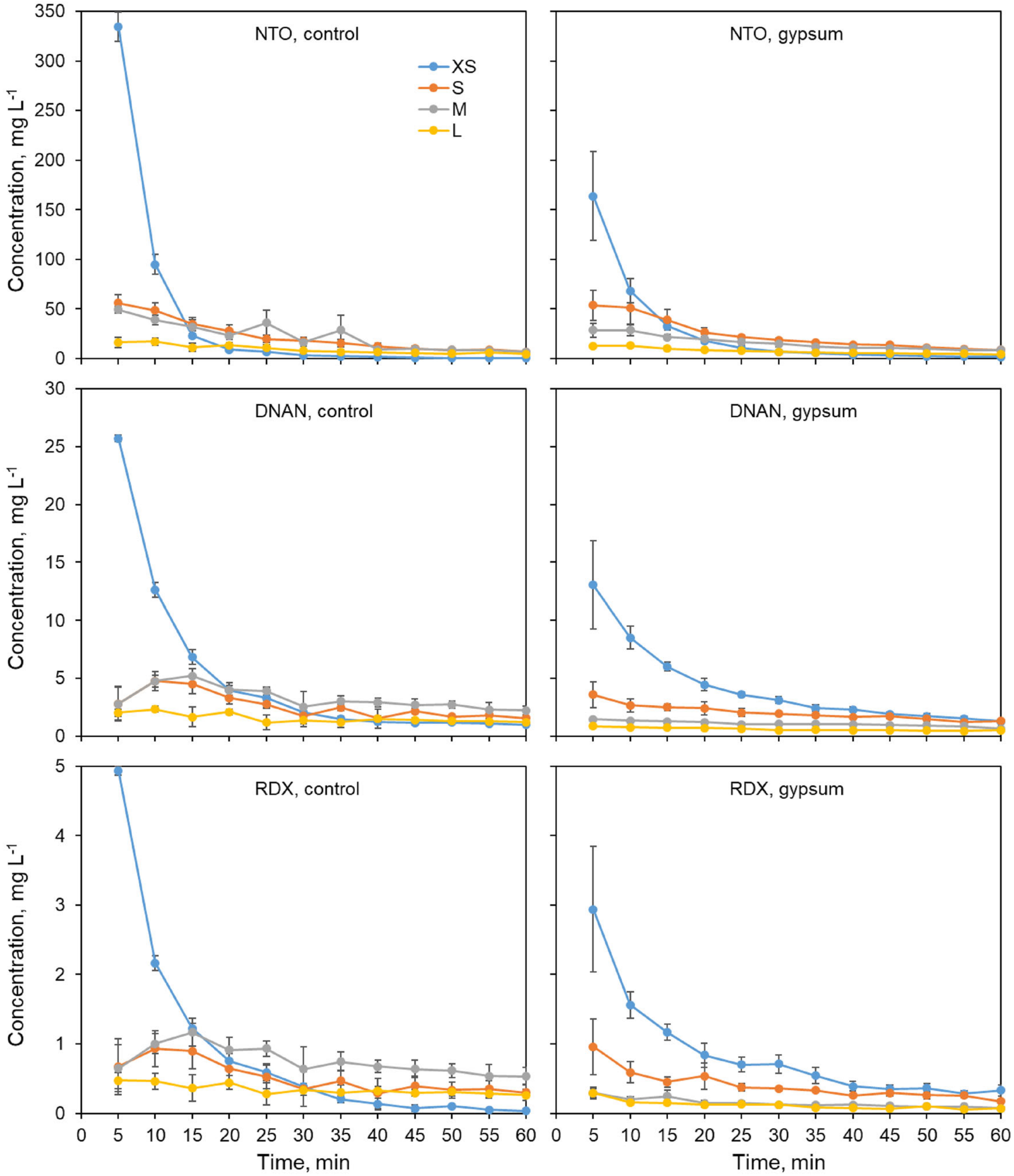

FIGURE 3 Concentrations of 3-nitro-1,2,4-triazol-5-one (NTO), 2,4-dinitroanisole (DNAN), and hexahydro-1,3,5-trinitro-1,3,5-triazine (RDX) dissolved in runoff as a function of time on the control and gypsum treated plots with particles of insensitive munition explosive (IMX)-104 of four different sizes, 4.75–9.51 mm (large, L), 2.83–4.75 mm (medium, M), 2–2.83 mm (small, S), and <2 mm (extra small, XS). Error bars equal standard error, $n = 3$.

Application of gypsum also significantly decreased the total (cumulative) loss to runoff of dissolved DNAN, RDX, and HMX for M and L particles. No significant differences between the treatments were observed among these same compounds for S and XS particles or NTO for all particle sizes.

It should be noted that particles <2 mm in size presented the majority of deposited material during low-order detonation for 61 mm mortar rounds and about half for 81 mm rounds (Bigl et al., 2021). Therefore, their behavior is likely to dominate the overall fate of energetics following low-order detonation.

The movement of solid energetics on the plots was highly variable (Figure 4). Such behavior is attributed to the discrete nature of particulate matter subject to entrainment, transport, and deposition cycle when in shallow overland flow (Lisle et al., 1998). It was particularly noticeable in case of S- and M-sized IMX-104 particles which alternate

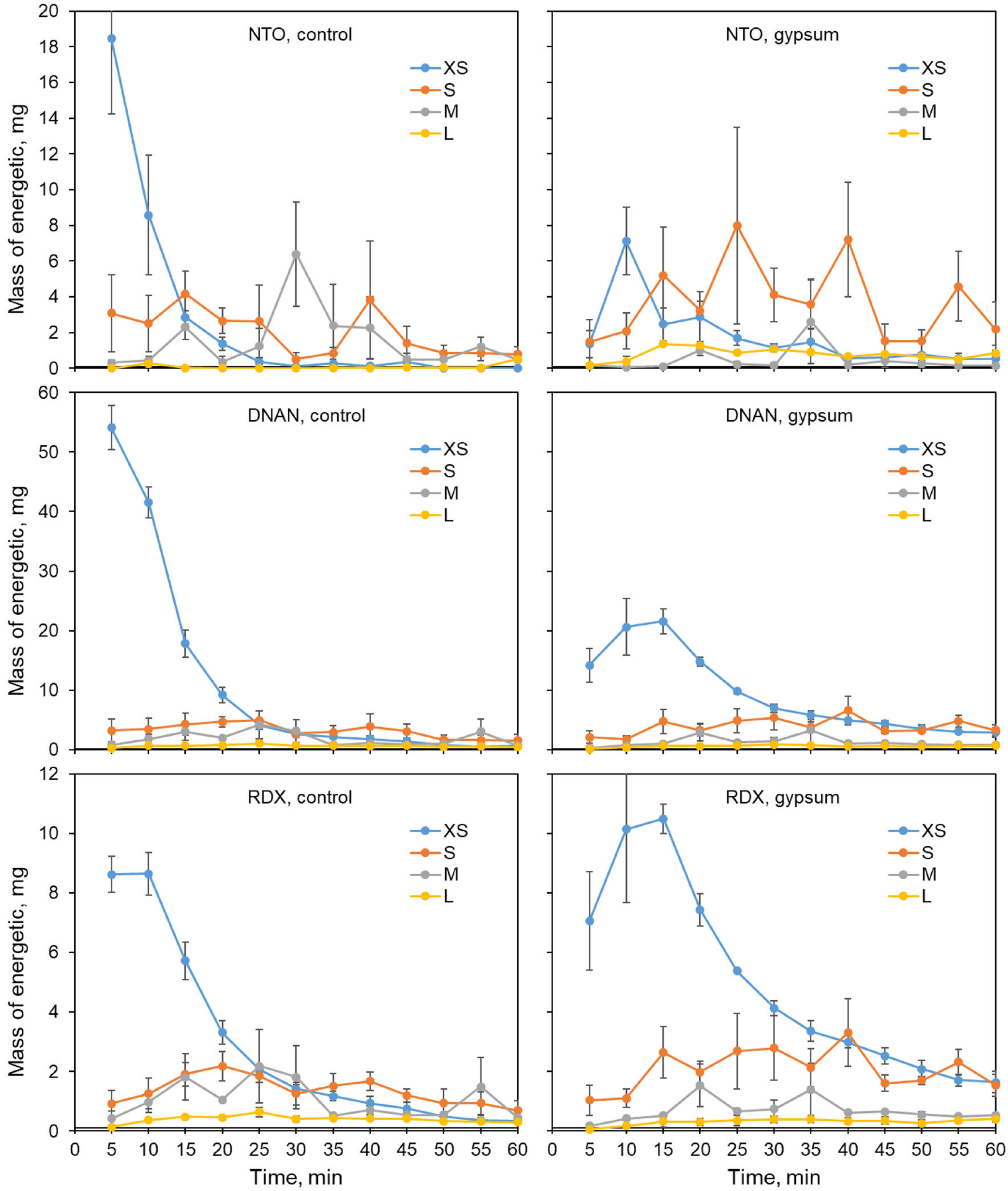

FIGURE 4 Concentrations of 3-nitro-1,2,4-triazol-5-one (NTO), 2,4-dinitroanisole (DNAN), and hexahydro-1,3,5-trinitro-1,3,5-triazine (RDX) in sediment as a function of time on the control and gypsum treated plots with particles of insensitive munition explosive (IMX)-104 of four different sizes, 4.75–9.51 mm (large, L), 2.83–4.75 mm (medium, M), 2–2.83 mm (small, S), and <2 mm (extra small, XS). Error bars equal standard error, $n = 3$.

between rest and motion resulting in stochastic nature of the transport.

The transport of XS particles exhibited early peak followed by a steady decline as their storage on the plot was being depleted. In contrast, L particles lacked mobility (Farenhorst & Bryan, 1995) and their measured yield from the plots could be attributed to breakup and flaking (Fuller et al., 2015; Wang et al., 2012). This was confirmed by comparing soil surface photographs before and after the event (Figure S1). Namely, after the rainfall L particles primarily remained in place, M were partially lost or moved, while S and XS were no longer found on the surface.

Gypsum affected the transport dynamic of XS energetic particles by decreasing and delaying their peak discharge (Figure 4). During the initial 5 min of simulation the yield of particulate NTO from XS gypsum plots (1.4 mg) was nearly

14-fold smaller than that from the control treatment (18.5 mg). The yield of particulate DNAN during the same time was also significantly smaller in gypsum (14.2 mg) than in the control (54.1 mg). In addition, gypsum caused the peak yield to shift from 5 to 15 min into the simulation for both NTO and DNAN. A similar time shift was observed for RDX, but without significant change in discharge rate. The impact of gypsum on larger particles was not significant. Delay in the peak of movement for energetic particles can have a significant impact on total transport. The rainfall in this study continued for 1 h, but under natural conditions shorter rains are more common and may never reach peak transport conditions.

In addition to the transport of explosives as particles, they can also be moved by runoff when adsorbed to the sediment. Transport of energetics adsorbed to the sediment was calculated before to be a minor contributor to overall fate of energetics during rainfall (Polyakov et al., 2023) due to low organic carbon content of Florence soil and relatively low sediment to water ratio in runoff (Table 1). It is expected that addition of gypsum would not affect adsorption coefficients for any of the constituents of IMX-104 in either bulk soil or suspended sediment. NTO adsorption is sensitive to soil pH (Mark et al., 2016b) as NTO gains negative charge at higher pH values (Nandi et al., 2013). However, pH of both soil (8.3) and gypsum solution (6.7) would result in negatively charged NTO, which is poorly adsorbed by negatively charged soils, as can be seen from low K_d values reported in Table 1. Adsorption of neutral compounds, such as DNAN, RDX, and HMX (Table 1), is not significantly affected by pH or ionic strength of the solution. Calculations showed that on gypsum treatment the amount of constituents transported adsorbed to sediment was 30% (NTO) to 50% (DNAN) less than on control (Table S1). This was due to both a decrease in solution concentration and lower sediment yield on plots with gypsum.

3.3 | Total IMX-104 mass balance

The total recovery rate of IMX-104 varied from 75% to 95% in the control and from 54% to 78% in the gypsum treatments. These rates were slightly lower but comparable to those reported by Crouch et al. (2020) for spiked aqueous and soil samples in laboratory conditions. There was no significant difference in recovery between the treatments except for L particles where it was lower on gypsum plots. There was also no relationship between recovery rate and particle size on either treatment.

The overall post rainfall mass balance of IMX-104 in the order from greater to smaller was as follows: (1) soil surface retention, (2) off-site loss to overland flow, and (3) sub-surface infiltration (Figure 5). Within the overland flow, the more soluble energetic NTO (Table 1) was primarily transported in dissolved form, while the less soluble compounds (DNAN, RDX, and HMX) were transported in particulate form. In addition, the ratio of dissolved to particulate mass depended on the energetic initial particle size and this ratio decreased from XS to L fraction.

The application of gypsum significantly decreased the total (cumulative) loss to runoff of dissolved DNAN, RDX, and HMX for M and L particles by 58%–79%. No significant differences between the treatments were observed among these same compounds for S and XS particles or NTO for any particle sizes (Figure 5). The infiltration pathway for NTO in gypsum was significantly greater than in the control. In addition, in gypsum less soluble DNAN and RDX (Table 1) were also present in infiltration, while in the control none were found. It appears that the effect of gypsum was to redirect mobilized energetics into the subsurface flow. However, when in soil, NTO has been shown to undergo biotransformation (Mark et al., 2016b, 2017) and complete biomineralization (Rios-Valenciana et al., 2023), which may offset potential negative groundwater effects.

The response of IMX-104 to rainfall impact was complex, due to the fact that munition residue is a distribution of various particle sizes (Bigl et al., 2020), while each particle is a physical mixture of components with different properties. In this mixture more soluble NTO is imbedded into the less soluble matrix of DNAN (Taylor et al., 2013). Once NTO starts to dissolve, the particle is more likely to break up, and that in turn triggers further rapid dissolution (Dontsova et al., 2023; Taylor et al., 2013). As a result, the effectiveness of gypsum amendment in mitigating IMX-104 redistribution and loss was dependent on the energetic compound, the initial particle size, and the transport pathway.

4 | CONCLUSIONS

The purpose of the study was to investigate the effect of gypsum amendment on redistribution of IMX-104 under the impact of rainfall. Addition of gypsum more than doubled the infiltration, although the effect on surface flow was not significant. The total sediment loss under gypsum decreased by 16% comparing to the control, while the overall dynamics of sediment transport also changed. A lower steady state sediment discharge was achieved quicker than in the control. These observations were consistent with previous research, indicating that the primary effect of gypsum is to inhibit soil dispersion caused by rain water and improve infiltration, impeding sediment loss.

The initial concentration in runoff of all energetic compounds (NTO, DNAN, RDX, and HMX) from XS particles was significantly lower (40%–77%) in the gypsum treatment than in the control. Presumably this happened due to a decrease in movement and dissolution of the smallest particles. As a result, in the gypsum treatment, it took longer for

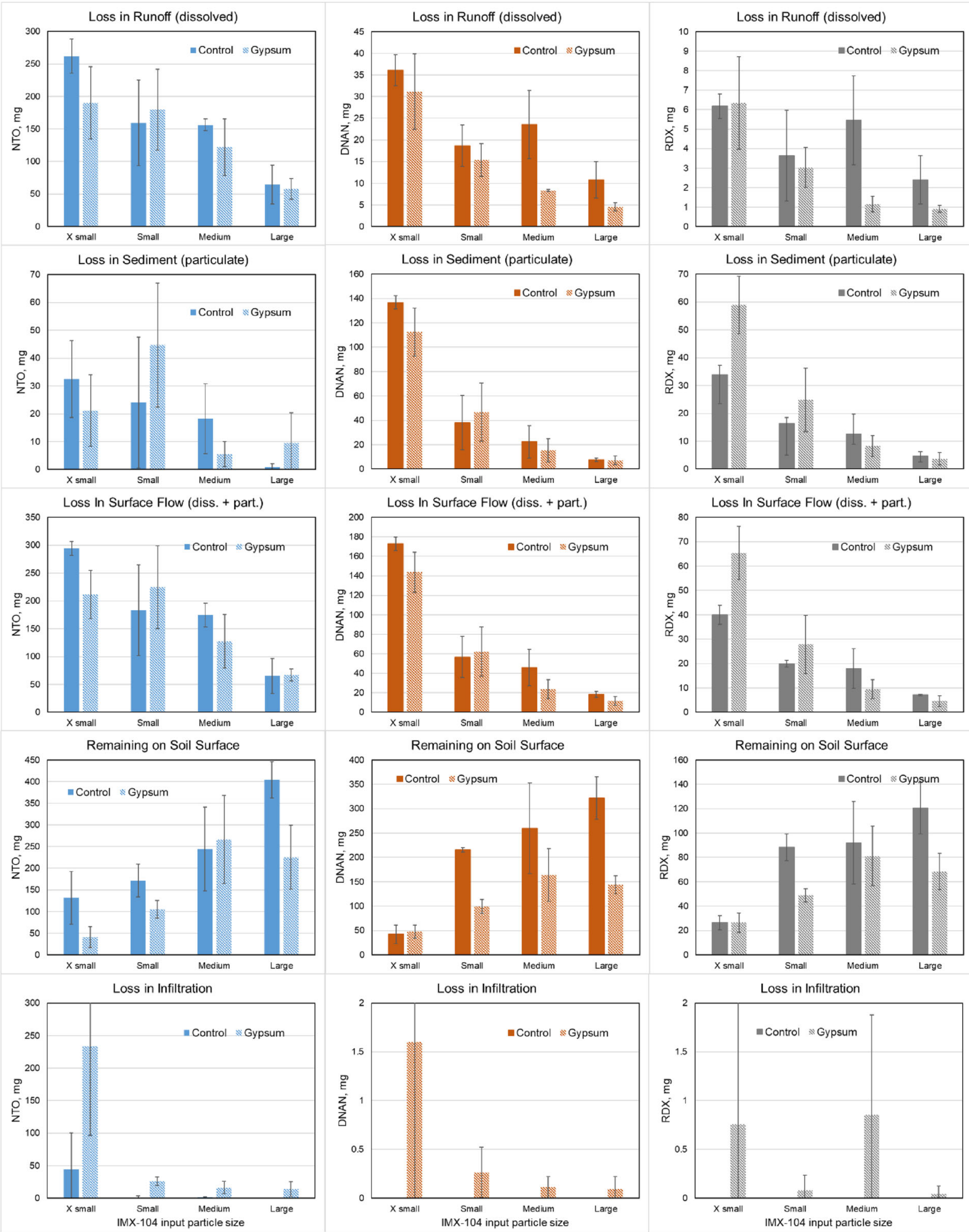

FIGURE 5 Comparison of insensitive munition explosive (IMX)-104 mass balance between two treatments (control and gypsum) by energetic component, transport pathway (runoff, sediment, soil surface, and infiltration), and particle size (standard error bars, $n = 3$).

concentrations in runoff to reach a steady state. Also, application of gypsum significantly decreased (NTO, DNAN, and HMX) and delayed (NTO, DNAN, RDX, and HMX) peak discharge of XS particulate energetics, while transport of S, M, and L particulates remained unaffected by the amendment.

After 50 mm of rainfall, which is equivalent to 5- to 10-years return frequency for Midwestern (Hershfield, 1961) and Southwestern (Polyakov et al., 2010) United States, of the total amount of IMX-104 placed on the plots most remained on the soil surface, with smaller amounts lost off-site in overland flow and transported with sub-surface infiltration. More soluble NTO (Table 1) tended to move off the plot in dissolved form, while the less soluble DNAN, DRX, and HMX moved in particulate form. The application of gypsum significantly decreased the total loss to runoff of dissolved DNAN, RDX, and HMX for M and L particles. Movement of NTO with infiltration in the gypsum treatment was fivefold greater than in the control. Moreover, DNAN and RDX were also present in infiltration, while in the control none were found. The effect of gypsum on the total balance was to redistribute more of the mobilized energetics into the subsurface flow.

The benefit of the gypsum treatment of IMX-104 contaminated soil needs further investigation since the energetics may follow different degradation processes depending on their transport pathway and terminal location.

ACKNOWLEDGMENTS

This study was funded through Strategic Environmental Research and Development Program (SERDP) under project ER19-1074. Authors are grateful to Dr. Andrea Leeson, Deputy Director & Environmental Restoration Program Manager, for continued support; Kim Birdsall for her help in collecting soils used in the experiments; and Matthew Bigl for providing the energetic residues.

AUTHOR CONTRIBUTIONS

Viktor Polyakov: Data curation; formal analysis; investigation; methodology; writing—original draft. **Samuel Beal**: Resources; writing—review and editing. **Stephen Mercer Meding**: Formal analysis; writing—review and editing. **Katerina Dontsova**: Conceptualization; formal analysis; funding acquisition; investigation; project administration; supervision; writing—review and editing.

CONFLICT OF INTEREST STATEMENT

The authors declare no conflicts of interest.

ORCID

Viktor Polyakov https://orcid.org/0000-0002-1452-0950

REFERENCES

Abrahams, A. D., & Parsons, A. J. (1994). Hydraulics of interrill overland flow on stone covered desert surfaces. *Catena*, *23*(1–2), 111–140. https://doi.org/10.1016/0341-8162(94)90057-4

Arthur, J. D., Mark, N. W., Taylor, S., Šimunek, J., Brusseau, M. L., & Dontsova, K. M. (2017). Batch soil adsorption and column transport studies of 2,4-dinitroanisole (DNAN) in soils. *Journal of Contaminant Hydrology*, *199*, 14–23. https://doi.org/10.1016/j.jconhyd.2017.02.004

ATSDR. (1997). *Toxicological profile for HMX*. U.S. Department of Health and Human Services, Public Health Service.

ATSDR (2012). *Toxicological profile for RDX*. U.S. Department of Health and Human Services, Public Health Service.

Beal, S. A., & Bigl, M. F. (2022). Particle size characteristics of energetic materials distributed from low-order functioning mortar munitions. *Journal of Energetic Materials*, 1–16. https://doi.org/10.1080/07370652.2022.2155730

Bigl, M. F., Beal, S. A., & Ramsey, C. A. (2021). *Determination of residual low-order detonation particle characteristics from IMX-104 mortar rounds* (ERDC/CRREL TR-21-12). US Army Corps of Engineers.

Bigl, M. F., Beal, S. A., Walsh, M. R., Ramsey, C. A., & Burch, K. M. (2020). Sieve stack and laser diffraction particle size analysis of IMX-104 low-order detonation particles (ERDC/CRREL TR-20-3). Cold Regions Research and Engineering Laboratory.

Boddu, V. M., Abburi, K., Maloney, S. W., & Damavarapu, R. (2008). Thermophysical properties of an insensitive munitions compound, 2,4-dinitroanisole. *Journal of Chemical and Engineering Data*, *53*(5), 1120–1125. https://doi.org/10.1021/je7006764

Bradford, J., Ferris, J., & Remley, P. (1987). Interrill soil erosion processes: I. Effect of surface sealing on infiltration, runoff, and soil splash detachment. *Soil Science Society of America Journal*, *51*(6), 1566–1571. https://doi.org/10.2136/sssaj1987.03615995005100060029x

Brannon, J., & Pennington, J. (2002). *Environmental fate and transport process descriptors for explosives* (Final report ERDC/EL TR-02-10). US, Army Corps Engineers, Engineer Research and Development Center, Environmental Laboratory.

Brooks, M. C., Davis, J. L., Larson, S. L., Felt, D. R., & Nestler, C. C. (2003). *Topical lime treatment for containment of source zone energetics contamination* (Final report ERDC/EL TR-03-19). Engineer Research and Development Center.

Charola, A. E., Pühringer, J., & Steiger, M. (2007). Gypsum: A review of its role in the deterioration of building materials. *Environmental Geology*, *52*, 339–352. https://doi.org/10.1007/s00254-006-0566-9

Crouch, R. A., Smith, J. C., Stromer, B. S., Hubley, C. T., Beal, S., Lotufo, G. R., Butler, A. D., Wynter, M. T., Russell, A. L., Coleman, J. G., Wayne, K. M., Clausen, J. L., & Bednar, A. J. (2020). Methods for simultaneous determination of legacy and insensitive munition (IM) constituents in aqueous, soil/sediment, and tissue matrices. *Talanta*, *217*, 121008. https://doi.org/10.1016/j.talanta.2020.121008

Dontsova, K., Brusseau, M., Kadoya, W., Qin, C., Hunt, E., Taylor, S., Beal, S. A., & Simunek, J. (2023). *Phototransformation, sorption, transport, and fate of mixtures of NTO, DNAN, and traditional explosives as a function of climatic conditions* (Final report ER-2727). Department of Defense Strategic Environmental Research and Development Program (SERDP). https://serdp-estcp.mil/projects/details/61df10c6-9ea4-4814-a8eb-47a8bce562bf/er-2727-project-overview

Dontsova, K., Taylor, S., Qin, C., Hunt, E., Brusseau, M., & Simunek, J. (2020). *Photo-transformation, sorption, transport, and fate of mixtures of NTO, DNAN, and traditional explosives as a function of climatic conditions* (ER-2727). SERDP & ESTCP.

Dontsova, K. M., Hayes, C., Pennington, J. C., & Porter, B. (2009). Sorption of high explosives to water dispersible clay: Influence of organic carbon, aluminosilicate clay, and extractable iron. *Journal of Environmental Quality*, *38*(4), 1458–1465. https://doi.org/10.2134/jeq220652008.0183

Dontsova, K. M., & Norton, L. D. (2002). Clay dispersion, infiltration, and erosion as influenced by exchangeable Ca and Mg. *Soil Science*, *167*(3), 184–193. https://doi.org/10.1097/00010694-200203000-00003

Farenhorst, A., & Bryan, R. B. (1995). Particle-size distribution of sediment transported by shallow flow. *Catena*, *25*(1–4), 47–62. https://doi.org/10.1016/0341-8162(94)00041-C

Favaretto, N., Norton, L., Joern, B., & Brouder, S. (2006). Gypsum amendment and exchangeable calcium and magnesium affecting phosphorus and nitrogen in runoff. *Soil Science Society of America Journal*, *70*(5), 1788–1796. https://doi.org/10.2136/sssaj2005.0228

Fuller, M. E., Schaefer, C. E., Andaya, C., & Fallis, S. (2015). Production of particulate composition B during simulated weathering of larger detonation residues. *Journal of Hazardous Materials*, *283*, 1–6. https://doi.org/10.1016/j.jhazmat.2014.08.064

Fuller, M. E., Schaefer, C. E., Andaya, C., Lazouskaya, V., Fallis, S., Wang, C., & Jin, Y. (2012). Dissolution kinetics of sub-millimeter composition B detonation residues: Role of particle size and particle wetting. *Chemosphere*, *88*(5), 591–597. https://doi.org/10.1016/j.chemosphere.2012.03.038

Gust, K. A., Lotufo, G. R., Stanley, J. K., Wilbanks, M. S., Chappell, P., & Barker, N. D. (2018). Transcriptomics provides mechanistic indicators of mixture toxicology for IMX-101 and IMX-104 formulations in fathead minnows (*Pimephales promelas*). *Aquatic Toxicology*, *199*, 138–151. https://doi.org/10.1016/j.aquatox.2018.03.019

Hawari, J., Monteil-Rivera, F., Perreault, N., Halasz, A., Paquet, L., Radovic-Hrapovic, Z., Deschamps, S., Thiboutot, S., & Ampleman, G. (2015). Environmental fate of 2, 4-dinitroanisole (DNAN) and its reduced products. *Chemosphere*, *119*, 16–23. https://doi.org/10.1016/j.chemosphere.2014.05.047

Hershfield, D. M. (1961). *Rainfall frequency Atlas of the United States for durations from 30 minutes to 24 hours and return periods from 1 to 100 years* (Technical paper no. 40). Cooperative Studies Section, Hydrologic Services Division for Engineering Division, Soil Conservation Service, USDA.

Karls, B., Meding, S. M., Li, L., Polyakov, V., Kadoya, W., Beal, S., & Dontsova, K. (2023). A laboratory rill study of IMX-104 transport in overland flow. *Chemosphere*, *310*, 136866. https://doi.org/10.1016/j.chemosphere.2022.136866

Kumar, A., & Saha, A. (2011). Effect of polyacrylamide and gypsum on surface runoff, sediment yield and nutrient losses from steep slopes. *Agricultural Water Management*, *98*(6), 999–1004. https://doi.org/10.1016/j.agwat.2011.01.007

Le Campion, L., Giannotti, C., & Ouazzani, J. (1999). Photocatalytic degradation of 5-nitro-1,2,4-triazol-3-one NTO in aqueous suspention of TiO2. Comparison with Fenton oxidation. *Chemosphere*, *38*(7), 1561–1570.

Lee, S., Gantzer, C., Thompson, A., & Anderson, S. (2010). Polyacrylamide and gypsum amendments for erosion and runoff control on two soil series. *Journal of Soil and Water Conservation*, *65*(4), 233–242. https://doi.org/10.2489/jswc.65.4.233

Lent, E. M. (2019). *Toxicology assessment of IMX-104* (S. 0012411b-18). US Army Public Health Center Aberdeen Proving Ground.

Li, L., Nearing, M., Polyakov, V., Nichols, M., & Cavanaugh, M. L. (2020). Evolution of rock cover, surface roughness, and flow velocity on stony soil under simulated rainfall. *Journal of Soil and Water Conservation*, *75*(5), 651–668. https://doi.org/10.2489/jswc.2020.00086

Lisle, I. G., Rose, C. W., Hogarth, W. L., Hairsine, P. B., Sander, G. C., & Parlange, J. Y. (1998). Stochastic sediment transport in soil erosion. *Journal of Hydrology*, *204*(1–4), 217–230. https://doi.org/10.1016/S0022-1694(97)00123-6

Lotufo, G. R., Stanley, J. K., Chappell, P., Melby, N. L., Wilbanks, M. S., & Gust, K. A. (2018). Subchronic, chronic, lethal and sublethal toxicity of insensitive munitions mixture formulations relative to individual constituents in Hyalella azteca. *Chemosphere*, *210*, 795–804. https://doi.org/10.1016/j.chemosphere.2018.07.049

Mark, N., Arthur, J., Dontsova, K., Brusseau, M., & Taylor, S. (2016). Adsorption and attenuation behavior of 3-nitro-1,2,4-triazol-5-one (NTO) in eleven soils. *Chemosphere*, *144*, 1249–1255. https://doi.org/10.1016/j.chemosphere.2015.09.101

Mark, N., Arthur, J., Dontsova, K., Brusseau, M., Taylor, S., & Šimůnek, J. (2017). Column transport studies of 3-nitro-1, 2, 4-triazol-5-one (NTO) in soils. *Chemosphere*, *171*, 427–434. https://doi.org/10.1016/j.chemosphere.2016.12.067

Miller, W. (1987). Infiltration and soil loss of three gypsum-amended Ultisols under simulated rainfall. *Soil Science Society of America Journal*, *51*(5), 1314–1320. https://doi.org/10.2136/sssaj1987.03615995005100050040x

Monteil-Rivera, F., Paquet, L., Deschamps, S., Balakrishnan, V. K., Beaulieu, C., & Hawari, J. (2004). Physico-chemical measurements of CL-20 for environmental applications: Comparison with RDX and HMX. *Journal of Chromatography A*, *1025*(1), 125–132. https://doi.org/10.1016/j.chroma.2003.08.060

Nandi, A. K., Singh, S. K., Kunjir, G. M., Singh, J., Mandal, A. K., & Pandey, R. K. (2013). Assay of the insensitive high explosive 3-nitro-1, 2, 4-triazol-5-one (NTO) by acid-base titration. *Central European Journal of Energetic Materials*, *10*(1), 113–122.

Norton, D., & Dontsova, K. (1998). Use of soil amendments to prevent soil surface sealing and control erosion. *Advances in GeoEcology*, *31*, 581–588.

Paige, G. B., Stone, J. J., Smith, J. R., & Kennedy, J. R. (2004). The walnut gulch rainfall simulator: A computer-controlled variable intensity rainfall simulator. *Applied Engineering in Agriculture*, *20*(1), 25–31. https://doi.org/10.13031/2013.15691

Parsons, A. J., Abrahams, A. D., & Luk, S. H. (1991). Size characteristics of sediment in interrill overland-flow on a semiarid hillslope, Southern Arizona. *Earth Surface Processes and Landforms*, *16*(2), 143–152. https://doi.org/10.1002/esp.3290160205

Peterson, J. R., Flanagan, D. C., & Tishmack, J. K. (2002). Polyacrylamide and gypsiferous material effects on runoff and erosion under simulated rainfall. *Transactions. of the ASAE*, *45*(4), 1011. https://doi.org/10.13031/2013.9912

Polyakov, V., Kadoya, W., Beal, S., Morehead, H., Hunt, E., Cubello, F., Meding, S. M., & Dontsova, K. (2023). Transport of insensitive munitions constituents, NTO, DNAN, RDX, and HMX in runoff and sediment under simulated rainfall. *Science of the Total Environment*, *866*, 161434. https://doi.org/10.1016/j.scitotenv.2023.161434

Polyakov, V., Stone, J., Holifield Collins, C., Nearing, M. A., Paige, G., Buono, J., & Gomez-Pond, R.-L. (2018). Rainfall simulation experiments in the southwestern USA using the Walnut Gulch Rainfall Simulator. *Earth System Science Data*, *10*(1), 19–26. https://doi.org/10.5194/essd-10-19-2018

Polyakov, V. O., Nearing, M. A., Nichols, M. H., Scott, R. L., Stone, J. J., & McClaran, M. P. (2010). Long-term runoff and sediment yields from small semiarid watersheds in southern Arizona. *Water Resources Research*, *46*. https://doi.org/10.1029/2009WR009001

Price, R. A., Bourne, M., Price, C. L., Lindsay, J., & Cole, J. (2011). *Transport of RDX and TNT from composition-B explosive during simulated rainfall*. American Chemical Society ACS Symposium Series.

Qin, C., Abrell, L., Troya, D., Hunt, E., Taylor, S., & Dontsova, K. (2021). Outdoor dissolution and photodegradation of insensitive munitions formulations IMX-101 and IMX-104: Photolytic transformation pathway and mechanism study. *Chemosphere*, *280*, 130672. https://doi.org/10.1016/j.chemosphere.2021.130672

Rios-Valenciana, E. E., Menezes, O., Blubaum, C., Romero, J., Krzmarzick, M. J., Sierra-Alvarez, R., & Field, J. A. (2023). Biodegradation of the emerging contaminant 3-nitro-1, 2, 4-triazol-5-one and its product 3-amino-1, 2, 4-triazol-5-one in perlite/soil columns. *Chemosphere*, *335*, 139121. https://doi.org/10.1016/j.chemosphere.2023.139121

Schwarzenbach, R. P., Gschwend, P. M., & Imboden, D. M. (2003). *Activity coefficient and solubility in water, environmental organic chemistry*. John Wiley & Sons.

Shainberg, I., Sumner, M., Miller, W., Farina, M., Pavan, M., & Fey, M. (1989). Use of gypsum on soils: A review. In B. Stewart (Ed.), *Advances in soil science* (pp. 2–111). Springer-Verlag.

Singh, S., Jelinek, L., Samuels, P., Di Stasio, A., & Zunino, L. (2010, October 11–14). *IMX-104 characterization for DoD qualification* [Paper presentation]. 2010 Insensitive Munitions & Energetic Materials Technology Symposium, Munich, Germany.

Sokkalingam, N., Potoff, J. J., Boddu, V. M., Maloney, S. W., & Baird, J. (2008). Prediction of environmental impact of high-energy materials with atomistic computer simulations (ADM002187). In *Proceedings of the 26th Army Science Conference* (pp. 1–4). Defense Technical Information Center.

Taylor, S., Dontsova, K., Walsh, M. E., & Walsh, M. R. (2015). Outdoor dissolution of detonation residues of three insensitive munitions (IM) formulations. *Chemosphere*, *134*, 250–256. https://doi.org/10.1016/j.chemosphere.2015.04.041

Taylor, S., Lever, J. H., Fadden, J., Perron, N., & Packer, B. (2009). Simulated rainfall-driven dissolution of TNT, Tritonal, Comp B and Octol particles. *Chemosphere*, *75*(8), 1074–1081.

Taylor, S., Ringelberg, D. B., Dontsova, K., Daghlian, C. P., Walsh, M. E., & Walsh, M. R. (2013). Insights into the dissolution and the three-dimensional structure of insensitive munitions formulations. *Chemosphere*, *93*(9), 1782–1788. https://doi.org/10.1016/j.chemosphere.2013.06.011

Torbert, H. A., & Watts, D. B. (2014). Impact of flue gas desulfurization gypsum application on water quality in a coastal plain soil. *Journal of Environmental Quality*, *43*(1), 273–280. https://doi.org/10.2134/jeq220652012.0422

Truman, C., Nuti, R., Truman, L., & Dean, J. (2010). Feasibility of using FGD gypsum to conserve water and reduce erosion from an agricultural soil in Georgia. *Catena*, *81*(3), 234–239. https://doi.org/10.1016/j.catena.2010.04.003

Tucker, W. A., Murphy, G. J., & Arenberg, E. D. (2002). Adsorption of RDX to soil with low organic carbon: Laboratory results, field observations, remedial implications. *Soil and Sediment Contamination: An International Journal*, *11*(6), 809–826.

USEPA. (2006). *SW846 Method 8330b: Nitroaromatics, nitramines, and nitrate esters by high performance liquid chromatography (HPLC)*. Office of Solid Waste and Emergency Response.

Wallace, B., Norton, L., & Woodward, R. (2001). Erosion control by amending soil with synthetic gypsum. In *10th International Soil Conservation Organization Conference Proceedings* (pp. 1158–1162). USDA-ARS.

Walsh, M., Thiboutot, S., & Gullette, B. (2017). *Characterization of residues from the detonation of insensitive munitions* (SERDP Project ER-2219). Strategic Environmental Research and Development Program (SERDP).

Walsh, M. R., Walsh, M. E., Ramsey, C. A., Thiboutot, S., Ampleman, G., Diaz, E., & Zufelt, J. E. (2014). Energetic residues from the detonation of IMX-104 insensitive munitions. *Propellants, Explosives, Pyrotechnics*, *39*(2), 243–250. https://doi.org/10.1002/prep.201300095

Wang, C., Fuller, M. E., Schaefer, C. E., Fu, D., & Jin, Y. (2012). Modeling the dissolution of various types of mixed energetic residues under different flow conditions. *Journal of Hazardous Materials*, *235*, 138–143. https://doi.org/10.1016/j.jhazmat.2012.07.035

Yoon, J. M., Oh, B.-T., Just, C. L., & Schnoor, J. L. (2002). Uptake and leaching of octahydro-1, 3, 5, 7-tetranitro-1, 3, 5, 7-tetrazocine by hybrid poplar trees. *Environmental Science & Technology*, *36*(21), 4649–4655. https://doi.org/10.1021/es020673c

Yoon, J. M., Oliver, D. J., & Shanks, J. V. (2005). Plant transformation pathways of energetic materials (RDX, TNT, DNTs). In A. Eaglesham (Ed.), *Agricultural biotechnology: Beyond food and energy to health and the environment* (pp. 103–116). NABC.

Zhang, X. C., Miller, W. P., Nearing, M. A., & Norton, L. D. (1998a). Effects of surface treatment on surface sealing, runoff, and interrill erosion. *Transactions of the ASAE*, *41*(4), 989–994. https://doi.org/10.13031/2013.17271

Zhang, X. C., Nearing, M. A., Norton, L. D., Miller, W. P., & West, L. T. (1998). Modelling interrill sediment delivery. *Soil Science Society of America Journal*, *62*(2), 438–444. https://doi.org/10.2136/sssaj1998.03615995006200020021x

Zhu, B., & Alva, A. (1994). The effect of gypsum amendment on transport of phosphorus in a sandy soil. *Water, Air, and Soil Pollution*, *78*, 375–382. https://doi.org/10.1007/BF00483044

Zoca, S. M., & Penn, C. (2017). An important tool with no instruction manual: A review of gypsum use in agriculture. *Advances in Agronomy*, *144*, 1–44. https://doi.org/10.1016/bs.agron.2017.03.001

SUPPORTING INFORMATION

Additional supporting information can be found online in the Supporting Information section at the end of this article.

How to cite this article: Polyakov, V., Beal, S., Meding, S. M., & Dontsova, K. (2025). Effect of gypsum on transport of IMX-104 constituents in overland flow under simulated rainfall. *Journal of Environmental Quality*, *54*, 191–203. https://doi.org/10.1002/jeq2.20652